LASERS

PACS numbers: 42.55.Px; 42.60.Da
DOI: 10.1070/QE2005v035n08ABEH008995

Theory of a vertical-cavity surface-emitting semiconductor laser with an external mirror

D.V. Vysotskii, A.P. Napartovich

Abstract. **High-power lasing in a single spatial mode of a vertical-cavity surface-emitting semiconductor laser (VCSEL) can be achieved by controlling the mode composition by means of an external cavity. Among the important factors which affect the mode composition is the interference of the fields inside the VCSEL and the field which returns after reflection from the external mirror. An approximate theoretical analysis of the optical modes is performed for a VCSEL with an external mirror. The mode frequencies and the degree of longitudinal mode discrimination are determined in a plane wave approximation. A condition for the existence of a single longitudinal mode is obtained. A two-dimensional equation for the effective refractive index is derived in the explicit form, which describes the transverse field distributions. Explicit expressions are obtained for the fields of transverse modes in a VCSEL with a plane external mirror and a parabolic profile of the gain.**

Keywords: *semiconductor laser, external cavity, vertical cavity*.

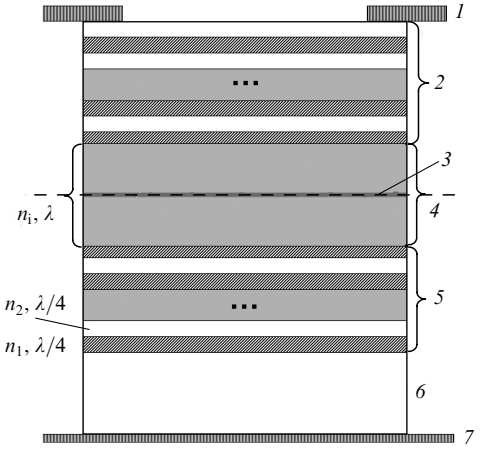

Figure 1. Scheme of a VCSEL: (*1*, *7*) contacts; (*2*, *5*) Bragg mirrors (BM); (*3*) active layer consisting of several quantum wells; (*4*) Λ layer; (*6*) substrate.

1. Introduction

Vertical-cavity surface-emitting semiconductor lasers (VCSELs), which were developed 25 years ago [1], have found wide use due to a perfect beam quality and their small size [2]. These qualities are achieved due to the design of these lasers, which include highly reflecting Bragg mirrors (BMs) made up of a large number of quarter-wave layer pairs (Fig. 1). Single-mode VCSELs with an output power of ~ 10 mW and above would be advantageous as telecommunication transmitters or radiation sources for optical communications. However, presently available commercial VCSELs [3] possess an output power in the 3 – 5 mW range at a wavelength $\lambda = 0.85$ μm. These VCSELs have a small aperture of the built-in waveguide (diameter up to 3.5 μm) limited by an oxide layer.

The small aperture radius is responsible for a high electrical resistance and a high current density, which substantially impairs the laser reliability. Increasing the radiating aperture would allow lowering the heating and attaining a higher stable output power. The condition for the rejection of higher transverse waveguide modes leads to the appearance of a relationship between the jump of the refractive index at the waveguide boundary and the aperture dimension. The admissible jump decreases with increasing the aperture, reducing the level of intermode discrimination. Furthermore, the role of nonlinear self-focusing and thermal radiation focusing increases. To minimise the influence of nonlinear effects, a relatively big jump of the refractive index is required, i.e., a small aperture.

From the standpoint of obtaining a high-power single-mode lasing, structures with an antiwaveguide profile of the refractive index show considerable promise [4 – 6]. However, for aperture diameters above 8 μm, to achieve a substantial discrimination against the higher modes, it is necessary to employ more complex structures, such as resonant arrays of antiguides [7], antiresonant reflecting optical waveguides [8], or photonic crystals [9].

A high output power was recently obtained from surface-emitting semiconductor lasers with a composite cavity (Fig. 2): a VCSEL with an extended cavity [10], a VCSEL with one BM and a spherical mirror some distance away from it [11 – 14], and a VCSEL with an external mirror [15 – 17]. In particular, an output power as high as 500 mW for a beam quality $M^2 < 1.2$ was achieved in a VCSEL with an external mirror upon optical [12] and current [16] pumping. At the same time it is well known that optical feedback may result in changes in the spectrum [18] as well

D.V. Vysotskii, A.P. Napartovich State Scientific Center of the Russian Federation, Troitsk Institute for Innovation and Fusion Research, 142190 Troitsk, Moscow region, Russia; e-mail: dima@triniti.ru

Received 5 May 2005
Kvantovaya Elektronika **35** (8) 705 – 710 (2005)
Translated by E.N. Ragozin

as in polarisation [19] and intensity [20] instability of the output radiation. In particular, numerical simulations [20] of the oscillation dynamics of a laser with a three-mirror cavity, which models a VCSEL with an external mirror, demonstrated the possibility of transition to chaotic oscillation with increasing the feedback factor. To acquire a deeper understanding of the effect of an external mirror on the mode settling in a VCSEL, it is therefore desirable to develop simplified theoretical concepts.

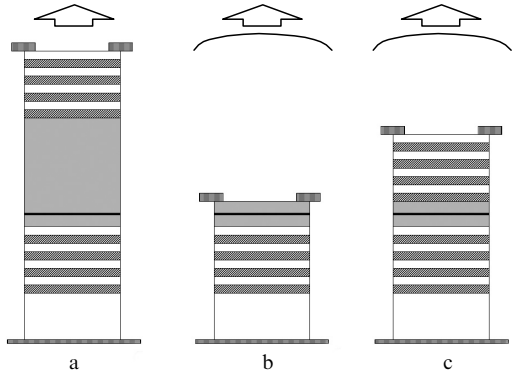

Figure 2. VCSELs with a compound cavity – extended (a), with one BM and a spherical mirror some distance away from it (b), and with an external mirror (c). The direction of the radiation output may vary.

The VCSEL designs optimised in efficiency and intermode discrimination are usually found by numerical methods. The employment of a rigorous finite-difference time domain method [21] results in a large body of time-consuming computations even for simple structures. For a VCSEL with an external mirror, the use of this method is quite often made difficult because of large geometrical dimensions. In [22], a method of the effective refractive index was proposed for the VCSEL calculation, which is based on approximate separation of variables in the longitudinal and transverse directions. The range of applications of this method was also determined.

It was shown in [23, 24] that a Bragg mirror is equivalent, as regards paraxial beam diffraction, to a plane mirror some distance away from the BM. The expression for this distance in the case of an arbitrary number of layer pairs with an arbitrary jump of the refractive index in the BM was derived in Ref. [25]. It was also proposed there to replace, in the paraxial approximation, a VCSEL with a plane–parallel cavity in which plane mirrors spaced at a distance equal to the effective VCSEL cavity length are placed instead of the Bragg mirrors. This length is defined as the sum of the distance between the BMs and the equivalent diffraction lengths for both BMs. In reality, the transverse VCSEL structure contains, as a rule, additional elements which limit the mode dimension, which leads to the necessity of substantiating the equivalent cavity technique.

In Ref. [26], a VCSEL with an extended monolithic cavity was analysed by representing the field distribution in the equivalent cavity as the sum of Laguerre–Gauss beams with an adjustable diameter.

We analyse the counter-propagating beam technique within the framework of the algorithm employed in Ref. [27]. The existence of small parameters (a low BM contrast and a small damping constant of the VCSEL cavity) permits obtaining simple expressions for effective VCSEL cavity lengths [28, 29]. In Ref. [30] we performed a numerical investigation of the transverse radiation modes of the VCSEL with an external mirror and formulated an approach to the approximate description of the transverse modes of such a cavity. In the present paper, we outline a consistent derivation of the effective refractive index model for a VCSEL with an external mirror, analyse the uniqueness conditions for the longitudinal mode, and derive explicit expressions for transverse-mode profiles in the case of a parabolic gain profile.

2. Equivalent cavity model for a VCSEL

The approach we elaborate is conveniently demonstrated by the example of a VCSEL without an external mirror. For a basis we take the method for determining cavity modes which involves the solution of the eigenvalue problem for the round-trip transit operator, which has been employed in laser physics beginning with the pioneering works of Fox and Li [31]. We consider a simplified version of VCSEL structure (Fig. 1) consisting of two BMs and a layer with an optical path length Λ equal to one radiation wavelength in between (the Λ layer). The active layer, which normally has several quantum wells, is replaced with an amplitude–phase screen in the middle of the Λ layer. The round-trip transit operator incorporates a reflection from the upper Bragg mirror, a passage through the Λ layer, a reflection from the lower Bragg mirror, and a passage through the Λ layer in the opposite direction. The propagation through a plane-lamellar structure of the waves with an in-vacuum wave number $k = \omega/c$ is described by the resolution of the radiation field into the plane waves with a transverse wave number $k_\perp$.

The authors of Ref. [25] obtained in the paraxial approximation the expression for the field reflection coefficient for a BM consisting of N quarter-wave layer pairs. In the subsequent discussion we restrict ourselves to the limiting case of mirrors with a low-contrast profile of the refractive index and retain only the first-order terms in the field expansion in terms of $\delta n/n$, where $\delta n = n_2 - n_1$ is the jump of the refractive index, $n = (n_1 n_2)^{1/2}$, and n_1 and n_2 are the lower and higher refractive indices of the quarter-wave layers, respectively. In this limit, the expression for plane-wave reflection coefficient R_N as a function of transverse wave number $k_\perp$ and the deviation δk from the resonance value k is of the form

$$R_N = \tanh(N\Psi)\left[1 - \mathrm{i}\left(\frac{\delta k}{k} - \frac{k_\perp^2}{2k^2n^2}\right)\frac{\pi \tanh(N\Psi)n}{\delta n}\right]^{-1}, \quad (1)$$

where

$$\Psi \approx \left(1 + \frac{k_\perp^2}{k^2n^2}\right)\frac{\delta n}{n} - \left(\frac{\delta k}{k}\right)^2 \frac{\pi^2 n}{2\delta n}$$

is the Bloch wave decrement; for simplicity, the refractive index of the medium around the mirror is taken to be equal to n_2. For a perpendicular incident plane wave with a resonance frequency ($\delta k = 0$, $k_\perp = 0$), the reflectivity increases with the number N of layer pairs and asymptotically tends to unity. The denominator of expression (1) defines the phase of R_N, correct to the principal small parameters included.

It is easy to see that the BM may, under the above assumptions, be replaced with a plane mirror with the reflection coefficient $\tanh(N\Psi)$, which is located some distance away from the BM surface. At the same time, from relationship (1) it follows that the phase of the BM reflectivity exhibits different dependences on the frequency detuning and the angle of incidence of the plane wave, so that two different equivalent lengths should be used. Namely, the length $L_\tau = \lambda n/(4n_2\delta n)$ is introduced for a normally incident plane wave [23], which characterises the phase shift $2L_\tau n_2 \delta k$ in the reflection from the BM. The equivalent diffraction length $L_D = \lambda n_2/(4n\delta n)$ is introduced to describe diffraction [24] such that, upon the transformation of the radius of curvature of a Laguerre–Gauss beam, the radiation propagation through this length and back is equivalent to the reflection from the BM.

In the general case, the medium on both sides of a BM has arbitrary refractive indices and even a simplified expression for the reflection coefficient (1) becomes cumbersome. If we restrict ourselves to the case of a BM with a high reflection coefficient realised in practice and denote the respective refractive indices of the input and output layers by n_i and n_e, we obtain

$$R_N = 1 + i\pi\left(\frac{\delta k}{k} - \frac{k_\perp^2}{2k^2n^2}\right)\frac{n_2 n}{n_i \delta n} - \frac{2t_N n_e}{n_i}, \qquad (2)$$

where $t_N = \exp(-2N\delta n/n) \ll 1$.

In the approach under consideration, the active layer at the centre of the Λ layer is replaced with a phase screen with a complex phase shift $\Phi(\boldsymbol{r})$ such that $||\Phi(\boldsymbol{r})| \ll 1$ (where $\boldsymbol{r}$ is the coordinate in the plane of the active layer). In this case, the screen position relative to the longitudinal mode profile should be taken into account (see, for instance, Ref. [30]). For a symmetric structure, taking this into account doubles the integral gain. The round-trip transit operator is the product of the BM reflection coefficients and the Λ-layer transmission coefficients. The BM reflection coefficients and the Λ-layer transmission coefficients are proportional to $\exp\{i[n_i\delta k\Lambda + \Phi(\boldsymbol{r})]\}$ and are close to unity, and their product is therefore represented as the sum of unity and small terms. If we go over to the coordinate space, the BM reflection coefficient is written as the following operator:

$$R_N = 1 - \frac{2t_N n_e}{n_i} + i\pi\,\frac{n}{\delta n}\,\frac{n_2}{n_i}\left(\frac{\delta k}{k} - \frac{\Delta_\perp}{2k^2n^2}\right), \qquad (3)$$

where $\Delta_\perp$ is the Laplace operator, which acts on the coordinates in the horizontal plane. The condition for field restoration after the round-trip transit path reduces to that the sum of small terms is equal to zero. By grouping in expression (3) the terms proportional to δk and $\Delta_\perp$, it can be shown that the equation for a VCSEL is structurally coincident with the equation for the modes of a homogeneous waveguide. Unlike the latter, however, in the equation there appear two cavity lengths for the VCSEL structure under consideration: the diffraction $L_D^c = [1 + nn_i/(2\delta n n_1)]\lambda n_i^{-1}$ and phase $L_\tau^c = [1 + nn_2/(2n_i\delta n)]\lambda n_i^{-1}$ lengths. In this case, the equation for the field $u(\boldsymbol{r})$ in the VCSEL takes on the following form (for simplicity, the number of layer pairs in the lower mirror is taken to be infinite):

$$\frac{\Delta_\perp u(\boldsymbol{r})}{2k^2n_i^2} + \left[\frac{\Phi(\boldsymbol{r}) + it_N n_e/n_i}{kn_i L_D^c} + \frac{L_\tau^c}{L_D^c}\,\frac{\delta k}{k}\right]u(\boldsymbol{r}) = 0. \qquad (4)$$

Eqn (4) corresponds to the effective refractive index approximation proposed for a VCSEL in Ref. [22]. Our approach shows that to $\Phi(\boldsymbol{r}) \equiv 0$ there corresponds an effective refractive index $n_{eff} = n_i(L_\tau^c/L_D^c)^{1/2}$. In this case, its profile is explicitly expressed in terms of the complex phase shift Φ in the phase screen (arising from the variations of the gain and refractive index in the plane of the active layer):

$$\frac{\delta n_{eff}}{n_{eff}} = \frac{\delta\lambda}{\lambda} = \frac{\Phi}{kn_i L_\tau^c}.$$

The imaginary term in Eqn (4) corresponds to radiation losses through the upper BM. Therefore, the use of effective refractive index technique is really justified in the paraxial approximation for a VCSEL with low-contrast BMs. Earlier [29] it was shown that for more complex VCSEL structures, the frequency shift of the fundamental mode agrees to within 5 %–10 % with the data obtained by numerical techniques.

3. Longitudinal modes of a VCSEL with an external mirror

Consider the longitudinal structure of a VCSEL with a plane external mirror (Fig. 3). The VCSEL consists of the lower and upper BMs, which are made up respectively of N_L and N_U layer pairs with a contrast $\delta n/n$, and the active Λ layer with an integral gain G intervening between them. The external mirror is located at a distance L from the upper BM and possesses a field reflection coefficient R_M, the space between the upper BM and the external mirror is filled with a material with $n = n_e$.

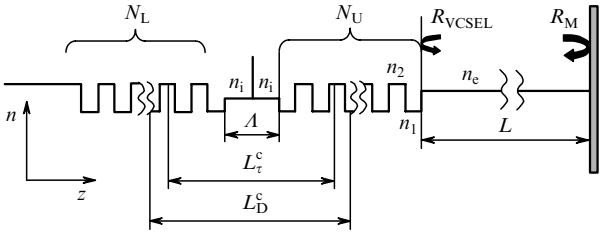

Figure 3. Scheme of a one-dimensional model of a VCSEL with an external mirror.

The resonance wavelength of VCSEL cavity is usually [32] determined from the reflection spectrum of the VCSEL cavity, which has a deep dip at the resonance. The practically used structures [16] have an antireflection coating on the upper BM, and therefore the reflection from the output surface of the upper BM on the side of external mirror can be neglected. A simple expression for the VCSEL near-resonance reflection coefficient in the case of a low-contrast BM can be written as

$$R_{VCSEL} = \frac{R_L - R_U + 2iR_L R_U \delta k n_i L_\tau^c + 2GR_U}{1 - R_L R_U - 2G - i\delta k n_i L_\tau^c (R_L + R_U)}, \qquad (5)$$

where $R_L = \tanh N_L\delta n/n$ and $R_U = \tanh N_U\delta n/n$ are the reflection coefficients at the resonance frequency for the

lower and upper BMs, respectively. The reflection coefficient of a passive VCSEL cavity at the resonance frequency ($\delta k = 0$) is $\tanh[(N_L - N_U)\delta n/n]$, i.e. is equal to zero for similar BMs ($N_L = N_U$), so that a symmetric VCSEL is transparent at the resonance frequency.

A VCSEL with an external mirror is a special case of a three-mirror cavity, whose longitudinal mode spectrum has been investigated in many papers. However, the characteristic property of the VCSEL is the existence of one longitudinal mode selected by the overlap of the field and amplification domains. In the plane-wave approximation, the dispersion equation for the VCSEL with an external mirror

$$R_{\mathrm{VCSEL}} R_{\mathrm{M}} \exp(2\mathrm{i}kn_{\mathrm{e}}L) = 1 \tag{6}$$

with the help of formula (5) is reduced to the following transcendental equation for the frequency detuning

$$y = \frac{R\chi}{1+R} \frac{\sin[2(y-w)]}{1+R\cos[2(y-w)]} \frac{n_{\mathrm{e}}L}{n_{\mathrm{i}}L_\tau^{\mathrm{c}}}, \tag{7}$$

where $y = \delta k n_{\mathrm{e}} L$; $R = |R_{\mathrm{M}}|$; $2w = \arg[R_{\mathrm{M}} \exp(2\mathrm{i}kn_{\mathrm{e}}L)]$ is the phase shift for the resonance-frequency wave in its passage from the upper BM to the external mirror and back. The following conditions were assumed to be fulfilled in the derivation of this equation: $\chi = (1 - R_{\mathrm{U}}) \ll 1$ (the upper BM has a high reflectivity), $R_{\mathrm{L}} = 1$ (the lower BM has an infinite number of layers), $\delta k n_{\mathrm{i}} L_\tau^{\mathrm{c}} \ll 1$ (the phase shift in tracing around the VCSEL arising from the frequency difference from the resonance one).

The graphic solutions of Eqn (7) are intersections of the straight line and the dashed curve in Fig. 4a for $w = 0$ (the wave returning to the VCSEL turns out to be in phase with the radiated wave) and in Fig. 4b for $w = \pi/2$ (the wave returning to the VCSEL and the radiated wave are oppositely phased). The threshold gain (Fig. 4, the solid curve) is determined from Eqn (6) using the formula

$$G = \frac{1 - R\cos[2(y-w)]}{1 + R\cos[2(y-w)]} \frac{\chi}{2}. \tag{8}$$

One can see from Fig. 4a that if the external cavity has a longitudinal mode exactly corresponding to the VCSEL mode ($w = 0$), the threshold gain is minimal: $G_{\min}^{\mathrm{th}} = \chi(1-R)/[2(1+R)]$. When the external cavity is short enough, for $w = 0$ there exists a single solution of Eqn (7). As the external cavity length is increased, new intersection points will appear in Fig. 4a. In the limit of a long external cavity, the modes closest to the resonance one possess the lowest oscillation threshold and the phase shift in the external cavity $2y \to \pm 2\pi$. The discrimination of these modes relative to the fundamental mode can be estimated as $\delta G_0 = [\pi L_\tau^{\mathrm{c}}(1+R)]^2/(2\chi^2 L^2 R)$. With increase in the parameter w (a tuned-out external cavity), the straight line in Fig. 4a shifts to the right to raise the threshold gain of the central mode. Furthermore, there appear neighbouring modes, whose lasing threshold lowers.

The limiting case ($w = \pi/2$) is considered in Fig. 4b. The mode with the resonance frequency ($\delta k = 0$) now possesses the highest threshold gain $G_{\max}^{\mathrm{th}} = \chi(1+R)/[2(1-R)]$. For a mirror with a reflectivity of 0.9 this signifies a 100-fold rise in the threshold gain. Two neighbouring modes ($y \approx \pm\pi/2$) have the same threshold gain $G_1^{\mathrm{th}} = G_{\min} + \delta G_0/4$ in the limit of long L. The oscillation threshold and the intermode discrimination for an arbitrary value of w will lie in the ranges defined by the two limits considered above.

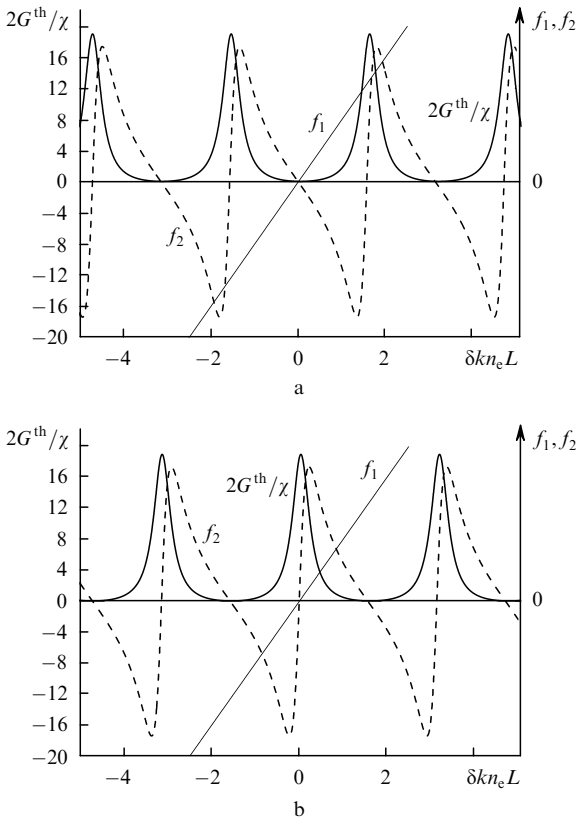

Figure 4. Graphic solution of Eqn (7) for $w = 0$ (a) and $\pi/2$ (b). Straight line (f_1) [the left-hand side of Eqn (7)], the dashed curve (f_2) [the right-hand side of Eqn (7)], the solid curve represents the ratio between the threshold gain and the upper BM transmittance. The reflectivity of external mirror is $R = 0.9$, $\chi n_{\mathrm{e}} L/(n_{\mathrm{i}} L_\tau^{\mathrm{c}1}) = 2$.

By analysing the situation when the straight line in Fig. 4 is tangent to the dashed curve, from Eqn (7) it is possible to derive the condition for the oscillation of a single longitudinal mode:

$$\frac{L}{L_\tau^{\mathrm{c}}} < \frac{n_{\mathrm{i}}(1-R^2)}{2\chi n_{\mathrm{e}} R}. \tag{9}$$

Therefore, the equivalent cavity model yields the conditions for the onset of oscillations and the degree of longitudinal mode discrimination in a VCSEL with a plane external mirror.

4. Transverse modes of a VCSEL with an external mirror

When a VCSEL with a plane external mirror has one longitudinal mode [the external cavity is tuned to the VCSEL cavity resonance, $w = 0$, and condition (9) is fulfilled], the technique for calculating the transverse VCSEL mode described in Section 2 can be generalised by adding to the round-trip transit operator of a compound cavity the operator of propagation to the external mirror and back with the inclusion of reflection. In the general case, the field of the wave returning to the VCSEL upon tracing around the external cavity is expressed with the help

of an integral operator in terms of the field emitted into the external cavity. The condition for the field restoration upon tracing around the compound cavity is therefore reduced to an integro-differential equation for the field emitted by the VCSEL:

$$u(r) = \hat{R}_{\mathrm{VCSEL}} \int\int \Gamma_{-}(L, \boldsymbol{r} - \boldsymbol{r}_{\mathrm{M}}) R_{\mathrm{M}}(\boldsymbol{r}_{\mathrm{M}}) \times \Gamma_{+}(L, \boldsymbol{r}_{\mathrm{M}} - \boldsymbol{r}') u(\boldsymbol{r}') \mathrm{d}\boldsymbol{r}' \mathrm{d}\boldsymbol{r}_{\mathrm{M}}, \quad (10)$$

where $\Gamma_{\pm}(z, \boldsymbol{r})$ are the field propagators in the external cavity by a distance z in the forward and backward directions, respectively; $\boldsymbol{r}_{\mathrm{M}}$ is the two-dimensional radius vector of a point on the mirror; the operator $\hat{R}_{\mathrm{VCSEL}}$ of reflection from the VCSEL is defined by formula (5) with replacement of $\delta k n_{\mathrm{i}} L_{\tau}^{\mathrm{c}}$ by the expression $\delta k n_{\mathrm{i}} L_{\tau}^{\mathrm{c}} - L_{\mathrm{D}}^{\mathrm{c}} k^{-2} n_{\mathrm{i}}^{-2} \Delta_{\perp}$. Eqn (10) is too complicated even in the case of a plane external mirror, when the nucleus of the integral operator is proportional to $\exp[\mathrm{i}k(\boldsymbol{r} - \boldsymbol{r}')^2 (4L)^{-1}]$, and calls for additional assumptions to obtain easily analysable solutions. The beam spreading in the external cavity over a distance short in comparison with the Rayleigh length $L_{\mathrm{R}}^{(a)} = \pi n_{\mathrm{e}} a^2/\lambda$ (where a is the beam radius) is insignificant. When the condition $L \ll L_{\mathrm{R}}^{(a)}$ is fulfilled, the inclusion of field distribution variation in tracing around the external cavity reduces to redefining the effective lengths. If we introduce the effective lengths of the compound cavity $L_{\tau}^{\mathrm{cl}} = L_{\tau}^{\mathrm{c}} + n_{\mathrm{e}} L\chi/(2n_{\mathrm{i}})$ and $L_{\mathrm{D}}^{\mathrm{cl}} = L_{\mathrm{D}}^{\mathrm{c}} + n_{\mathrm{i}} L\chi/(2n_{\mathrm{e}})$, from Eqn (10) it is possible to derive the equation for the model of effective refractive index

$$\frac{\Delta_{\perp} u(\boldsymbol{r}, t)}{2k^2 n_{\mathrm{i}}^2} + \left[\frac{L_{\tau}^{\mathrm{cl}}}{L_{\mathrm{D}}^{\mathrm{cl}}} \frac{\delta k}{k_0} + \frac{\Phi(\boldsymbol{r}) - \mathrm{i}(G - G_{\min})}{k n_{\mathrm{i}} L_{\mathrm{D}}^{\mathrm{cl}}} \right] u(\boldsymbol{r}, t) = 0. \quad (11)$$

The difference between Eqns (11) and (4) is that the effective VCSEL lengths are replaced with the effective lengths of the compound cavity. At the same time, it follows from Eqn (11) that increasing the length of external cavity decreases the jump of effective refractive index and lessens the effect exerted on the field mode by the inhomogeneities in the active layer described by the function $\Phi(\boldsymbol{r})$.

Near the oscillation threshold, the radial dependence gain can be approximated by a parabola $G = G_0(1 - r^2/\rho^2)$. When $\Phi(\boldsymbol{r}) = 0$, the solutions of Eqn (11) are Laguerre–Gauss functions of a complex argument. In this case, the fundamental mode is a Gaussian beam with an intensity profile proportional to $\exp(-r^2/r_1^2)$. The beam radius is $r_1 = [\rho^4/(N_{\mathrm{F}} G_0)]^{1/4}$, where $N_{\mathrm{F}} = k n_{\mathrm{i}} \rho^2 / L_{\mathrm{D}}^{\mathrm{cl}}$ is the Fresnel number of the compound cavity. The mode field localisation in a bounded region is known [32] to result in the blue shift of its eigenfrequency. In our case, this shift is $\delta k = (G_0/N_{\mathrm{F}})^{1/2} (n_{\mathrm{i}} L_{\tau}^{\mathrm{cl}})^{-1}$. As the external cavity length increases, the radius r_1 increases to ρ for $N_{\mathrm{F}} = G_0^{-1}$. The threshold gain of the fundamental mode $G_0^{\mathrm{th}} = G_{\min} + 1/(2N_{\mathrm{F}}) + [G_{\min} N_{\mathrm{F}}^{-1} + (2N_{\mathrm{F}})^{-2}]^{1/2}$ is also found from Eqn (11). The condition that the distance to the external mirror is short compared to the Rayleigh length for a beam of radius r_1 reduces, for the mode obtained, to the condition $L \ll L_{\mathrm{R}}^{(\rho)}$, where $L_{\mathrm{R}}^{(\rho)} = k n_{\mathrm{e}} \rho^2$ is the Rayleigh length for a beam of radius ρ.

The higher transverse modes are Laguerre–Gauss functions of a complex argument: $u(r, \varphi) = r^m \times L_n^{(m)}[(1 - \mathrm{i}) r^2/r_1^2] \exp[-(\mathrm{i}/2)^{1/2} r^2/r_1^2 + \mathrm{i}m\varphi]$, where m and n are the angular and radial beam indices, respectively. In this case, the parameter r_1 for them is the same as for the fundamental mode and the mode frequency shift to the blue is $m + 2n + 1$ time longer than for the fundamental mode. The transverse mode nearest to the fundamental mode in losses is the mode with $m = 1$, $n = 0$. The threshold gain for this mode is also explicitly calculated: $G_1^{\mathrm{th}} = G_{\min} + 2/N_{\mathrm{F}} + (4G_{\min} N_{\mathrm{F}}^{-1} + 4N_{\mathrm{F}}^{-2})^{1/2}$. Therefore, the degree of intermode discrimination lowers with increasing the Fresnel number of the cavity.

5. Conclusions

To acquire a deeper understanding of the mode formation mechanism in a VCSEL we have developed an analytic method for calculating the VCSEL cavity modes, which has enables us to derive a two-dimensional equation for the effective refractive index. In the plane-wave approximation, the frequencies of longitudinal modes and their oscillation thresholds were determined for a VCSEL with an external mirror. The condition for the oscillation of a single longitudinal mode was determined. The equation for the effective refractive index was generalised to the case of a VCSEL with an additional external mirror. The integro-differential equation reduces to a simple second-order equation when the plane external mirror is located at a distance much shorter than the Rayleigh length. We derived from this equation the spatial intensity profiles and oscillation thresholds of transverse modes in the case of a parabolic gain profile. The expressions obtained in this paper describe the principal parametric dependences of VCSEL mode characteristics.

Acknowledgements. This work was supported by the President of the Russian Federation (Grant No. NSh-794.2003.2) and the Russian Foundation for Basic Research (Grant No. 02-02-17101).

References

1. Soda H., Iga K., Kitahara C., Suematsu Y. *Jap. J. App. Phys.*, **18**, 2329 (1979).
2. Maleev N.A., Kuz'menkov A.G., Zhukov A.E., et al. *Fiz. Tekh. Poluprovodn.*, **39**, 487 (2005).
3. Jung C., Jager R., Grabherr M., Schnitzer P., Michalzik R., Weigl B., Muller S., Ebeling K.J. *Electron. Lett.*, **33**, 1790 (1997).
4. Choquette K.D., Hadley G.R., Hou H.Q., Geib K.M., Hammons B.E. *Electron. Lett.*, **34**, 991 (1998).
5. Wu Y.A., Li G.S., Nabiev R.F., Choquette K.D., Caneau C., Chang-Hasnain C.J. *IEEE J. Sel. Top. Quantum Electron.*, **1**, 629 (1995).
6. Oh T.H., McDaniel M.R., Huffaker D.L., Deppe D.G. *IEEE Photon. Techn. Lett.*, **10**, 12 (1998).
7. Bao L., Kim N.H., Mawst L.J., Elkin N.N., Napartovich A.P., Troshchieva V.N., Vysotsky D.V. *Appl. Phys. Lett.*, **84**, 320 (2004).
8. Zhou D.L., Mawst L.J. *IEEE J. Quantum Electron.*, **38**, 1599 (2002).
9. Furukawa A., Sasaki S., Hoshi M., Matsuzono A., Moritoh K., Baba T. *Appl. Phys. Lett.*, **85**, 5161 (2004).
10. Unold H.J., Mahmoud S.W.Z., Jaeger R., Kicherer M., Riedl M.C., Ebeling K.J. *IEEE Photon. Techn. Lett.*, **12**, 939 (2000).
11. Le H.Q., Di Cecca S., Mooradian A. *Appl. Phys. Lett.*, **58**, 1967 (1991).
12. Kuznetsov M., Hakimi F., Sprague R., Mooradian A. *IEEE J. Sel. Top. Quantum Electron.*, **5**, 561 (1999).

13. Nikolaeff F., Ballen T.A., Leger J.R., Gopinath A., Lee T.-C., Williams R.C. *Appl. Opt.*, **38**, 3030 (1999).
14. Tropper A.C., Foremann H.D., Garnache A., Wicox K.G., Hoogland S.H. *J. Phys D: Appl. Phys.*, **37**, R75 (2004).
15. Chen G.Q., Leger J.R., Gopinath A. *Appl. Phys. Lett.*, **74**, 1069 (1999).
16. McInerney J.G., Mooradian A., Lewis A., Shchegrov A.V., Strzelecka E.M., Lee D., Watson J.P., Liebman M., Carey G.P., Umbrasas A., Amsden C., Cantos B.D., Hitchens W.R., Heald D., Doan V.V. *Proc. SPIE Int. Soc. Opt. Eng.*, **4994**, 21 (2003).
17. Keeler G.A., Serkland D.K., Geib K.M., Peake G.M., Mar A. *IEEE Photon. Techn. Lett.*, **17**, 522 (2005).
18. Jiang S., Dagenais M., Morgan R.A. *IEEE Photon. Techn. Lett.*, **7**, 739 (1995).
19. Valle A., Pesquera L., Shore K.A. *IEEE Photon. Techn. Lett.*, **10**, 639 (1998).
20. Law J.Y., Agarwal G.P. *IEEE J. Sel. Top. Quantum Electron.*, **3**, 353 (1997).
21. Lee T.W., Hagness S.C., Zhou D., Mawst L.J. *IEEE Phot. Techn. Lett.*, **13**, 770 (2001).
22. Hadley G.R. *Opt. Lett.*, **20**, 1483 (1995).
23. Babić D.I., Corzine S.W. *IEEE J. Quantum Electron.*, **28**, 514 (1992).
24. Babić D.I., Chung Y., Dagli N., Bowers J.E. *IEEE J. Quantum Electron.*, **29**, 1950 (1993).
25. Riyopoulos S., Dialetis D., Ihnman J., Phillips A. *J. Opt. Soc. Am. B*, **18**, 1268 (2001).
26. Riyopoulos S., Unold H. *J. Lightwave Techn.*, **20**, 1173 (2002).
27. Zhou D., Mawst L.J., Napartovich A.P., Elkin N.N., Vysotsky D.V. *Proc. SPIE Int. Soc. Opt. Eng.*, **4649**, 168 (2002).
28. Napartovich A.P., Elkin N.N., Troshchieva V.N., Vysotsky D.V., Bao L., Zhou D., Kim N.H., Mawst L.J. *Proc. SPIE Int. Soc. Opt. Eng.*, **4994**, 112 (2003).
29. Elkin N.N., Napartovich A.P., Troshchieva V.N., Vysotsky D.V., Bao L., Kim N.H., Mawst L.J. *Laser Phys.*, **14**, 378 (2004).
30. Napartovich A.P., Elkin N.N., Troshchieva V.N., Vysotsky D.V. *Proc. SPIE Int. Soc. Opt. Eng.*, **5452**, 602 (2004).
31. Fox A.G., Li T. *Bell Syst. Techn. J.*, **40**, 453 (1961).
32. Chang-Hasnain C.J., in *Diode Laser Arrays*. Ed. by D. Botez, D.R. Scifres (Cambridge: Cambridge Univ. Press, 1994) pp 368 – 413.